



**CHALMERS**  
UNIVERSITY OF TECHNOLOGY

## **Effect of biomass ash on preventing aromatization of olefinic cracking products in dual fluidized bed systems**

Downloaded from: <https://research.chalmers.se>, 2023-01-21 01:06 UTC

Citation for the original published paper (version of record):

González Arias, J., Berdugo Vilches, T., Mandviwala, C. et al (2023). Effect of biomass ash on preventing aromatization of olefinic cracking products in dual fluidized bed systems. *Fuel*, 338. <http://dx.doi.org/10.1016/j.fuel.2022.127256>

N.B. When citing this work, cite the original published paper.



# Effect of biomass ash on preventing aromatization of olefinic cracking products in dual fluidized bed systems

Judith González-Arias<sup>\*</sup>, Teresa Berdugo-Vilches, Chahat Mandviwala, Isabel Cañete-Vela, Martin Seemann, Henrik Thunman

Department of Space, Earth and Environment (SEE), Division of Energy Technology, Chalmers University of Technology, 412 96 Gothenburg, Sweden

## ARTICLE INFO

### Keywords:

Dual fluidized bed  
Catalytic activation  
Ash-coated bed material  
Hydrocarbon cracking  
Biomass ash

## ABSTRACT

In this work, the effect of ash activated olivine on olefinic products cracking and aromatization was assessed. The experiments were carried out in the Chalmers 2–4 MW<sub>th</sub> dual fluidized bed gasifier, where the feedstock was cracked using steam as fluidization agent, at a reaction temperature of ca. 780–790 °C. Three activation states of the olivine, representing three consecutive days of the campaign, were evaluated. The changes of the permanent gas composition along with the reduction in aromatic species with the time of exposure to biomass ash demonstrate a clear effect of the ash activated olivine on the conversion of olefinic cracking products. The ash activation of the olivine clearly promoted the reactions involving steam. As a consequence, higher yields of permanent gases, mainly H<sub>2</sub>, CO and CO<sub>2</sub>, were produced at expenses of the yields of the total aromatic compounds and C<sub>4</sub> hydrocarbons and larger. It is concluded that the biomass ash activated olivine promotes the steam reforming path of the C<sub>4</sub> and larger hydrocarbon fragments, while avoiding the alternative aromatization route. The results presented here provide useful insights on the opportunities and limitations of ash activated materials in DFB systems when steam cracking linear hydrocarbon feedstocks, e.g., polyolefin-based materials.

## 1. Introduction

Olefins, mono aromatic hydrocarbons and syngas are valuable chemical building blocks in the chemical and petrochemical industry. These chemical compounds are traditionally produced from oil and gas, e.g., via steam cracking and catalytic cracking of naphtha, ethane or LPG and steam reforming of methane. In a context where there is a wish to decrease dependency on fossil fuels and to promote a circular economy, chemical building blocks can be alternatively recovered from plastic-rich waste streams. Direct steam cracking of plastic wastes in a dual fluidized bed (DFB) has been proven a suitable technology for this purpose [1,2].

A DFB gasifier consists of two interconnected fluidized bed reactors: a gasifier and a combustor. A sand-like material circulates between the reactors carrying the heat from the exothermic combustion zone to the endothermic gasification zone. The advantage of this type of configuration compared to a single bed gasifier is that in the DFB system the gasifier side can be fluidized with steam and avoid dilution of the product stream with N<sub>2</sub> and/or with flue gases. Additionally, the scheme of a DFB system allows synergies between feedstocks, for instance by co-

gasification [3–5] and by strategically feeding different feedstocks in the combustion and gasification sides. The latter arrangement is of interest when e.g., CO<sub>2</sub> emissions from the combustion side are only allowed if they are of biogenic origin, while other feedstocks can be applied in the gasification side to produce syngas and chemical building blocks [2]. In both cases, fossil-based feedstocks (e.g., plastic materials of fossil origin) and biomass are processed in the same DFB system.

Based on previous experiences with biomass fuels in large scale dual fluidized bed (DFB) gasifiers, it is known that over time-exposure to biomass ash the bed material acquires an ash layer [6,7]. The ash layer can exhibit catalytic properties when the bed material has a limited amount of silicon oxide content, e.g., olivine, bauxite, feldspar [8,9]. In systems handling biomass and plastic wastes simultaneously, the bed material will be thus exposed to biomass ash that can confer catalytic properties to the bed and influence the conversion of the plastic feedstock applied. Within the usual composition of woody biomass ash, the most reactive elements providing catalytic properties are calcium and potassium [8]. These ash elements are proven to interact with the bed material changing its physicochemical properties with time of exposure [10] and different layers with predominant species are usually identified

<sup>\*</sup> Corresponding author.

E-mail address: [Judith.gonzalez@chalmers.se](mailto:Judith.gonzalez@chalmers.se) (J. González-Arias).

over the bed material particles [11,12]. The catalytic activity of the bed material will thus be different with time as the ash layer develops, and simultaneously the bed material will be able to transport inorganic species between the reactors, e.g., sulphur [8], or potassium [13]. If the biomass ash contains transition metals, such as iron, a phenomenon referred to oxygen transport can occur. In this regard, oxides of transition metals act as oxygen carriers which oxidize with the air in the combustion side and get reduced by reacting with the feedstock in the gasifier [14]. Olivine is to date the bed material of choice in most large-scale DFB gasifiers due to its high acquired catalytic activity by interaction with biomass ash and its mechanical strength [11,15,16].

The steam cracking of plastic wastes in DFB results in a wide range of products including syngas (CO, CO<sub>2</sub> and H<sub>2</sub>), light hydrocarbons, monoaromatics, and polyaromatics (PAHs) [1,2]. The distribution of these groups and their corresponding yields highly depend on the chemical structure of the feedstock used and operating conditions [1]. Based on the experience with biomass, it is here hypothesized that the ash coating of the bed material can also alter the product distribution of the cracking of plastics. In the case of biomass, the ash-activated olivine limits the production of aromatics while shifting the product distribution towards syngas species (CO, CO<sub>2</sub> and H<sub>2</sub>) [12,16,17]. This effect has been explained by the reforming of the early precursors of aromatics through in-bed catalysis [18]. In biomass gasification, such precursors are to a large extent oxygenated species derived from the cracking of the cellulose and lignin structures. However, chemical structures very different from that of biomass can be found in plastic wastes, e.g., polyolefinic chains which are abundant in packaging items. In this case, the conditions for aromatization of the products are very different compared to the biomass case, as the polyolefins are linear, oxygen free and the cracking products are more concentrated in hydrocarbons.

The development of aromatic hydrocarbons from non-aromatic ones is inevitable in industrial steam cracking processes, and different hydrocarbons exhibit different tendencies to aromatization. For instance, methane and ethane have a very low probability of participation in the aromatics' formation; naphthenes show a high aromatization tendency; cyclic mono and diolefins are very effective precursors for aromatics; and alkynes have a much higher tendency to be converted into aromatics [19].

The thermal decomposition of polyolefinic hydrocarbons is typically described as a random scission process that consists of three steps: (1) initiation, where a radical is formed; (2) propagation, where both intra and intermolecular hydrogen transfer occurs; and (3) termination, where the free radicals are recombined to form paraffins, olefins and diolefins [20]. The yield and composition of the final cracking products are highly dependent on the operating conditions [21]. As simplified in Fig. 1, paraffins, olefins and diolefins that are produced in the primary cracking reaction can undergo secondary reactions, resulting in the

formation of light products that are richer in olefins. Other highly unsaturated products are also likely to form by dehydrogenation of olefins [20]. The dehydrogenation reactions to generate aromatic compounds, olefins and diolefins are responsible for H<sub>2</sub> formation at high temperatures [22–24]. When steam is used, additional H<sub>2</sub> can be produced from steam-related reactions such as steam reforming, Water-Gas-Shift (WGS), and steam gasification in case any char or carbon deposit are formed. These reactions are also sources of CO and/or CO<sub>2</sub>, although they seldom play a big role in the steam cracking process. In fact, steam is usually considered an inert diluting media in naphtha steam cracking [25].

The formation of aromatic compounds typically follows a consecutive reactions scheme. Reactions such as Diels and Alder reaction or cycloaddition can result in the formation of heavier products, which after a dehydrogenation process can form aromatic hydrocarbons, mainly benzene [26]. From a paraffin, small olefins are formed through cracking and hydrogen transfer. Then, higher olefins are formed via oligomerization, cracking and isomerization, to finally form the aromatics via cyclization and hydrogen transfer [27]. Previous works indicate that the yield of aromatics formed from olefins is higher than the corresponding one from paraffins. This means that the aromatization of paraffins involves a stage of dehydrogenation to the corresponding olefins [28]. These authors also suggest that the first step in the aromatization reaction is the cyclization of the paraffins and the olefins [28].

While it has been demonstrated that the ash-activated olivine can prevent the formation of aromatics from biomass, it is unclear if there is a similar effect on linear and oxygen-free structures. There are indications that species present in the biomass ash can have an impact on the aromatization of polyolefins. For instance, Song et al. showed a clear inhibiting effect of potassium on the aromatic's formation during cracking of olefins over a synthetic zeolite. The authors showed that the formation of benzene, toluene and other aromatic hydrocarbons decreased with the increase of the loading of potassium in the catalyst [29].

The aim of this work is to assess the influence of the ash-activated olivine on the aromatization route when cracking linear and oxygen free feedstock structures. In this work, the cracking of a polyolefinic material has been evaluated under steam cracking conditions in the presence of biomass ash. To assess the extent of aromatization, the yields of permanent gases and aromatic compounds produced are measured. Olivine, used as bed material, was activated by the continuous exposure to biomass ash over a 3-days campaign. The product distribution was characterized at three different states of activation, which correspond to the progressive activation of the bed material over three consecutive days of experimental campaign. This work is aimed at the product analysis starting from the basis that olivine gets activated when it gets in

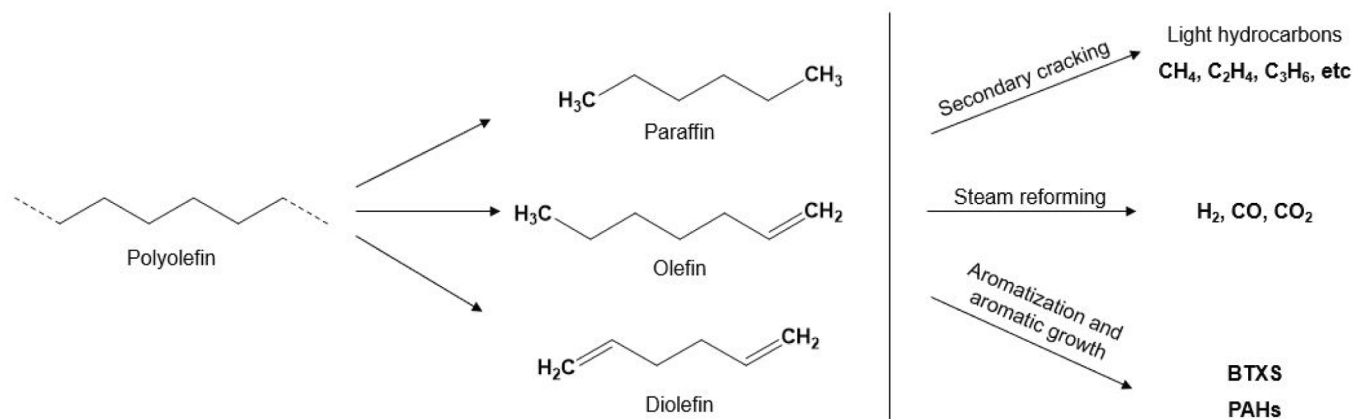


Fig. 1. Possible decomposition routes under steam cracking conditions.

contact with biomass ash in the combustor side as previously demonstrated by many authors [12,17,18,30,31]. The study of the ash layer formation and the distribution of the different ash elements over the ash layer is beyond the scope of this work. The reader is referred to the works of Faust et al. and Kuba et al. for a comprehensive characterization of the ash layer over olivine particles exposed to biomass ash in large DFB units [11,32,33].

## 2. Materials and methods

### 2.1. Experimental setup

The experiments were carried out in the DFB gasifier located at Chalmers University of Technology. This gasifier consists of a 2–4-MW<sub>th</sub> bubbling fluidized bed (BFB), coupled to a 12-MW<sub>th</sub> circulating fluidized bed (CFB) boiler. Fig. 2 shows a simplified layout of the system.

As can be seen in Fig. 2, the bed material circulates between the boiler (1) and the gasifier (6). The bed material coming from the boiler it is led to a cyclone (3) where the particulate matter is separated from the flue gas stream. This fraction is then collected in a transitional fluidized bed container or particle distributor (4). From here, it can either be introduced into the gasifier (6) or recirculated into the boiler. The bed material enters the gasifier through a loop seal (5) and thereafter, it returns to the boiler together with unconverted fuel via a second loop seal (7). Both the loop seals and the gasifier are fluidized with steam preventing gas leakage from the combustion side to the gasification side. Moreover, the raw gas produced via gasification is fed to the combustor to produce additional heat. Further details of the operation of the system

can be found elsewhere [34].

The experiments were carried out over 3 days of campaign, in which the olivine was continuously exposed to biomass ash in the boiler side of the DFB. One gasification test was carried out in each day of operation (Day 1, 2 and 3 respectively). Each gasification test could last several hours, in which measurement of the gasification products was carried out during a selected stable period. The olivine circulated within the system continuously during the 3-days period without any replacement or addition of new olivine (i.e., in continuous contact with biomass ash in the combustion side). To evaluate the effects of the olivine activation on the performance of the gasifier, similar operating conditions of the gasifier reactor were used during the 3 days of experiments. Small differences in the operating conditions are due to the difficulties and limitations in fine adjustment of a large plant. The main operational parameters used are listed in Table 1.

### 2.2. Materials

The elemental composition (wt.%) of the polyolefinic hydrocarbon used as feedstock was 85.63%wt. of carbon and 14.37%wt. of hydrogen. This feedstock has a linear molecular structure and does not contain ash. This would allow to assess the effect of the activation of the bed material with the ash of the biomass used in the combustion side without any interaction with the ash from the feedstock. The polyolefinic feedstock was fed in solid pellets from the top of the gasifier at the flows indicated in Table 1.

Olivine of Norwegian origin was employed as bed material. The average composition of the fresh olivine sand is shown in Table 2, while the particle density was measured in 3300 kg/m<sup>3</sup>. The bed inventory in the dual fluidized bed (DFB) system is approximately 2.5 – 3 tons. To provoke the formation of an active ash layer on the olivine particles, biomass was fed continuously to the combustor side during the 3-days campaign. The procedure was similar to what has been done in previous investigations focusing on the activation process [17].

Wood chips with the composition stated in Table 3 were applied and the biomass flow was 1.1 ton/h.

### 2.3. Gas measurements

The measurements presented in this work aim at characterising the composition of the raw gas produced in the gasifier side of the DFB unit. To quantify the total amount of dry gas produced per unit of feedstock, a small flow of helium was added as a tracer gas in the gasifier (~20 L<sub>N</sub>/min). The He stream is premixed with the fluidization steam before entering the gasifier. From the sampling point (blue cross in Fig. 2), a stream of raw gas is sampled continuously. This stream is used for the analysis of both aromatic compounds and permanent gases.

To measure the aromatic fraction produced in the cracking reaction, the solid-phase adsorption (SPA) method was employed. A detailed description of this method can be found elsewhere [35]. For each of the experimental cases evaluated, at least 3 SPA samples were taken. The identification and quantification of the aromatic compounds was done with a GC equipped with a flame ionization detector (GC-FID Bruker GC-450 and 430), which allows to identify species with boiling points from that of benzene to that of coronene. The GC-FID was calibrated for 27 species, and these are listed in Table 4.

Downstream of the SPA sampling port the gas stream is cooled down, filtered and analysed via gas chromatography. The instrument used to measure the permanent gas concentrations was a micro-GC (Varian CP4900). The micro-GC is equipped with a Poraplot Q and a MS5A columns, which used helium and argon as carrier gases, respectively. The gas was sampled and analysed every 3 min during a period of approximately 30–60 min when the operation was stable. The results presented here correspond to the average of the measurements carried out over each stable period, respectively. The gaseous species measured in the permanent gas fraction are He (tracer gas), H<sub>2</sub>, CO, CO<sub>2</sub>, CH<sub>4</sub>,

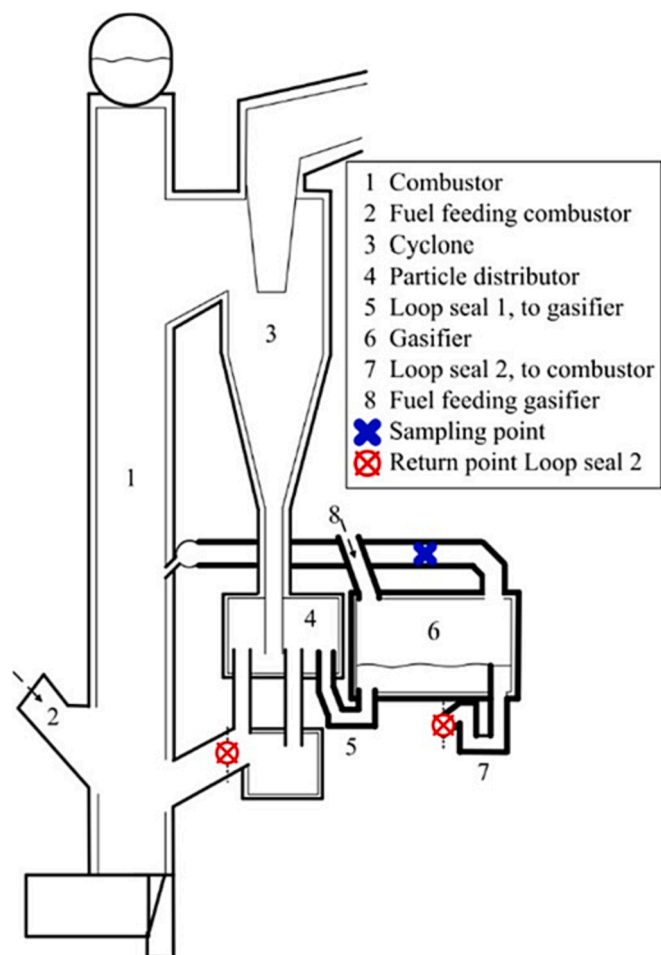


Fig. 2. Schematic layout of the Chalmers dual fluidized bed gasifier.

**Table 1**

Operational conditions used during the different tests.

Operational point	Temperature bed material (entrance of gasifier)	Temperature bed material (exit of gasifier)	Feedstock flow (kg/h)	Fluidization steam to gasifier (kg <sub>steam</sub> /h)	Average temperature bottom bed, boiler	Estimated gas velocity gasifier (m/s)
Day 1	788	781	132	160	840	3
Day 2	786	779	135	160	850	3
Day 3	782	776	120	160	858	3

**Table 2**

Composition of the olivine sand used as fresh bed material in this work. The percentages are presented in weight as received.

Metal oxide in olivine sand	% wt.
MgO	49.6
SiO <sub>2</sub>	41.7
Fe <sub>2</sub> O <sub>3</sub>	7.40
Al <sub>2</sub> O <sub>3</sub>	0.46
NiO	0.32
Cr <sub>2</sub> O <sub>3</sub>	0.31

**Table 3**

Elemental analysis and ash composition of the wood chips used in the combustor.

Elemental analysis	Value (wt.%, dry basis)
C	49.78
H	6.12
N	0.12
O	43.00
S	<0.02
Ash	0.70
LHV (MJ/kg, dry basis)	18.23
Ash composition	Value (mg/kg, dry basis)
Al	21
Si	91
Fe	21
Ti	1.4
Mn	70
Mg	231
Ca	1750
Ba	16.8
Na	43.4
K	910
P	91

**Table 4**

Calibrated species in GC-FID.

Group	Species included
1-ring	Benzene, toluene, o/p-xylene, styrene, methyl-styrene
2-rings	Naphthalene, indene, 1,2-dihydronaphthalene, methyl-naphthalene, biphenyl
>3-rings	Acenaphthylene, acenaphthene, fluorene, phenanthrene, anthracene, xanthene
≥4-rings	Fluoranthene, pyrene, chrysene
Phenols	Phenol, o/p-cresol, 1-naphthol, 2-naphthol
Furans	2,3-benzofuran, dibenzofuran

C<sub>2</sub>H<sub>2</sub>, C<sub>2</sub>H<sub>6</sub>, C<sub>3</sub>H<sub>6</sub>, N<sub>2</sub>, and O<sub>2</sub>.

The analysis is carried out in yields, i.e., in mols or grams per unit feedstock fed into the gasifier. Additionally, the yields of gas and aromatic compounds were used for the evaluation of the carbon, hydrogen and oxygen balances. The ambition with the analysis of the elemental balances was to understand the carbon balance closure, carbon distribution into the different products as well as the contribution of steam and eventual oxygen transport by the bed material in the reaction environment.

### 3. Results

#### 3.1. Activation and product distribution

As can be observed in Fig. 3, with the time of exposure, the edges of the olivine particles become smoother. In fact, considerable differences can be seen between Day 0 (olivine as received) and Day 3 as the particles are clearly more rounded due to attrition combined with ash depositions on the particle surfaces, which contribute to the ash layer formation as previously observed in refs [33,36]. SEM images showcased in Fig. 3 were taken at ca. 300 μm. At this point is important to highlight that a comprehensive study and characterization of the ash layer created over the particles is out of the scope of this work. For further information about the different elements found in the particles surface and their concentrations, the reader is referred to the work of Faust et al. [33]. In this work, a detailed investigation of the layer growth over olivine particles is shown at microscopic scale.

A clear evolution of the produced gas is also observed from Days 1 to 3. Fig. 4 shows the average yields of the permanent gases derived from the thermal decomposition of the polyolefinic feedstock obtained in the 3 days of operation respectively. The yield of H<sub>2</sub> increases by 25% from Day 1 to 2, and by 77% from Day 2 to Day 3. CO and CO<sub>2</sub> also show an important increase. When it comes to the light hydrocarbons, CH<sub>4</sub> and C<sub>2</sub>H<sub>4</sub> are the most abundant species, and their composition remains similar with a slight decreasing trend from Day 1 to 3. A similar slight decreasing trend is observed for C<sub>2</sub>H<sub>2</sub> although its yield is two orders of magnitude smaller compared to those of CH<sub>4</sub> and C<sub>2</sub>H<sub>4</sub>. In the case of C<sub>2</sub>H<sub>6</sub> and C<sub>3</sub> hydrocarbons a clear increasing trend can be seen as the exposure of olivine to biomass ash proceeds. Note that the presence of H<sub>2</sub>S in the raw gas evidences that sulphur was transported from the boiler to the gasifier side by means of the bed material, since no sulphur is presented in the gasifier feedstock while some sulphur is present in the wood chips fed to the boiler. Previous works indicate that the mechanism of sulphur transportation by the bed material can occur in the form of sulfates of alkali and alkali earth metals. In the bases of thermodynamic calculations and TEM-EDS analysis, Faust et al. showed the formation of K<sub>2</sub>Ca<sub>2</sub>(SO<sub>4</sub>)<sub>3</sub> and K<sub>2</sub>SO<sub>4</sub> over olivine particles activated in the same reactor than the one used in this work [33]. A possible reaction path for the release of H<sub>2</sub>S from the bed material in the gasifier involves the reaction of sulphur and potassium to form K<sub>2</sub>S, which reacts with steam in the gasifier releasing KOH and H<sub>2</sub>S [31]. It is therefore assumed that sulphur is transported in the form of sulphates reacting with other elements found also in the biomass ash (e.g., potassium or calcium).

The corresponding analysis of the aromatic compounds in Days 1–3 are summarized in Figs. 5 and 6. Fig. 5 shows the most abundant aromatic species measured, given an arbitrary cut at species that are present in an amount which is >3.5 g/kg feedstock. There most abundant species are benzene, toluene, styrene, indene and naphthalene, which together make up to 83%, 83% and 86% of the total measured aromatics in Days 1 to 3, respectively. At the temperature applied in this investigation, i.e., 780–790 °C, benzene is the most predominant aromatic compound at all stages of activation of the olivine. The share of benzene in the total aromatic mass detected was increasing from 50%, 51% and 55% during the three consecutive days, respectively. Fig. 6 summarizes the rest of aromatic compounds detected by GC-FID, where those that the instrument was not calibrated for are labelled as “unknown”. The detected but “unknown” aromatic species are a minor fraction of the

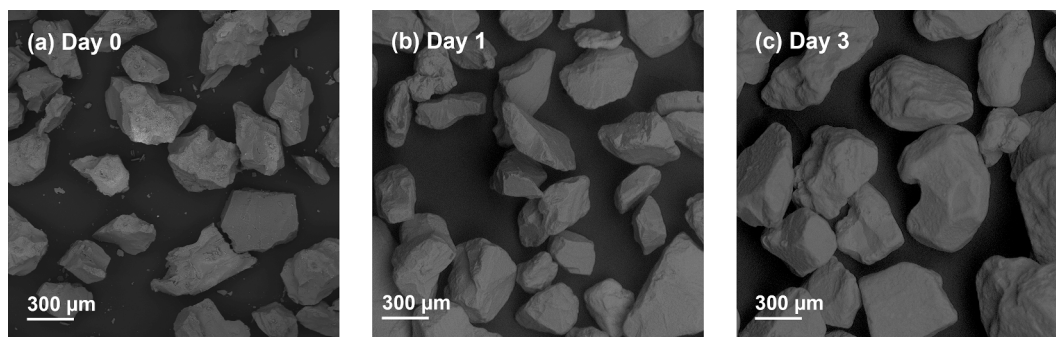


Fig. 3. Top-view micrographs of the olivine particles with the time of exposure.

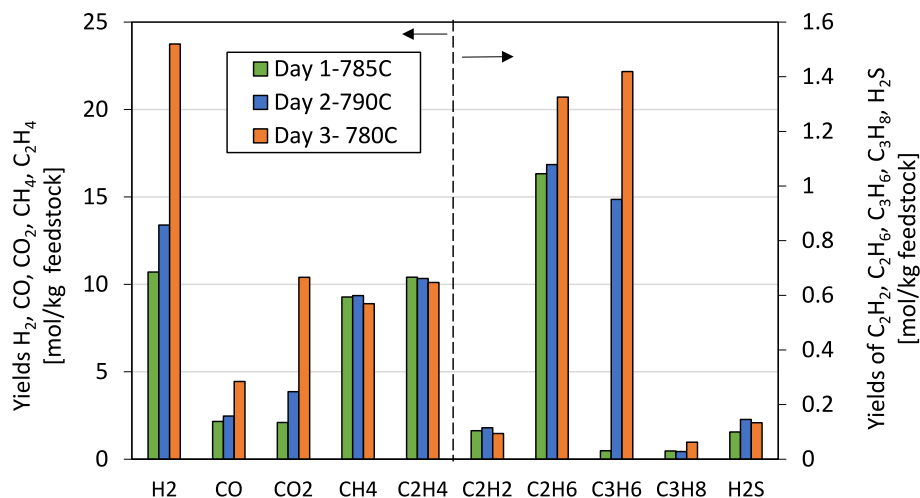


Fig. 4. Product yield in mol per kg of feedstock of the analysed gases after the steam cracking tests for the different days of activation.

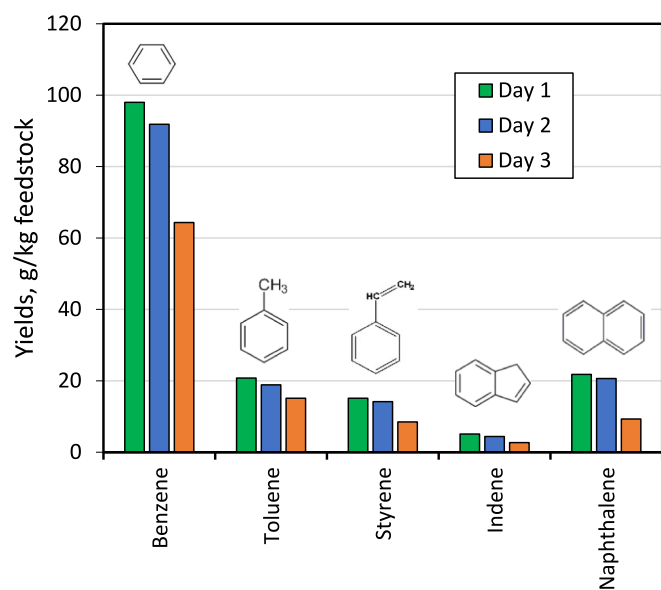


Fig. 5. Yields in g per kg of feedstock of the most abundant aromatic species (>3.5 g/kg) measured during the different days of activation.

total aromatics, i.e., 7%, 6% and 5% of the detected aromatic mass in Days 1–3, respectively.

From Day 1 to Day 3 the yields of aromatic species show a decreasing trend. The total aromatic yield for Day 2 was measured in 180 g/kg of

feedstock which represents a decrease of ca. 9% relative to Day 1. This reduction in aromatic yield reaches 41% when comparing the reference day (Day 1) to the day when the olivine was most activated (Day 3). When looking at each aromatic specie separately, the yields of all species decrease. Only two compounds (acenaphthylene and phenanthrene) follow a different trend, increasing during the first day of activation and visibly decreasing during the second one. This is in line with previous observations on the lower effect of the catalytic activity towards  $\geq 3$ -ring compounds [37].

Recall that during the three days of operation presented, the major change in the system is the time of exposure of the bed to the biomass fed to the gasifier. As shown in Table 1, the operational conditions for the 3 days of experiments are quite similar (i.e., feedstock and steam feeding rates and operating temperatures). And based on previous experiences in the Chalmers DFB system, we can conclude that a difference of 5 °C in the temperature of the gasifier makes only minor differences in the product distribution obtained [18]. Therefore, it can be inferred that the changes observed in the gas yields, along with the changes in olivine particle morphology confirm that the olivine became ash activated, as expected from previous experiences [6,11,30,38]. Therefore, the changes in reaction paths discussed hereinafter can be attributed predominantly to the effect of the ash layer formed on the olivine particles as it was intended.

### 3.2. Elemental carbon balance

For a better understanding and comparative analysis, the distribution of the carbon among the different products obtained in this process is presented in this section in Fig. 7. The figure represents the percentage of the carbon from the feedstock that leaves the gasifier in the form of

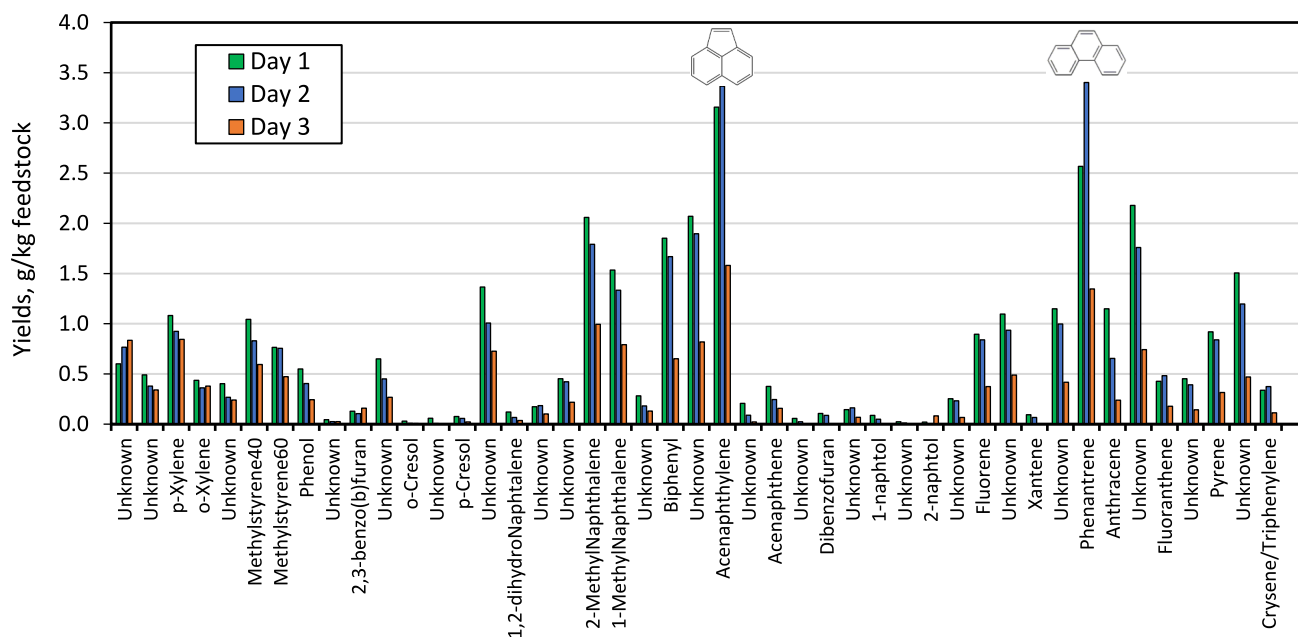


Fig. 6. Yields in g per kg of feedstock of measured aromatic species (<3.5 g/kg) during the different days of activation.

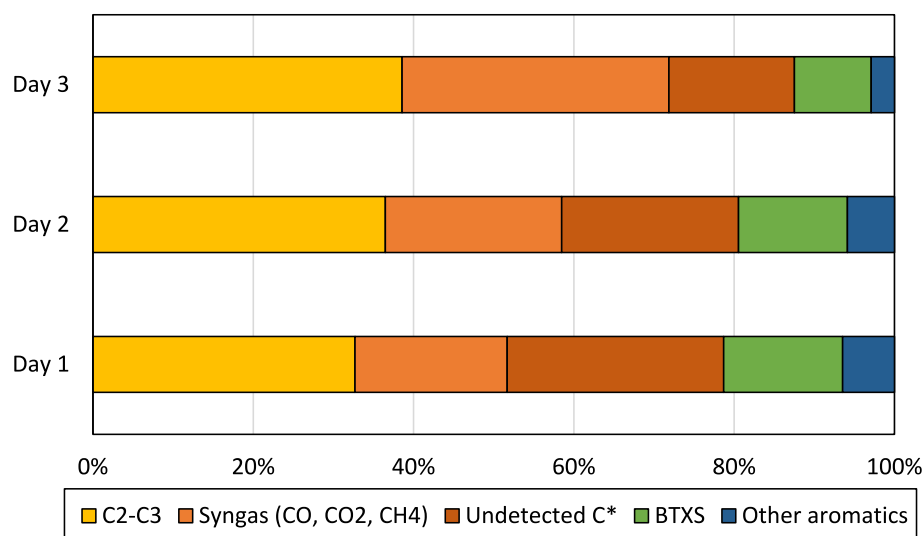


Fig. 7. Distribution of the carbon into gasification products during the aging process of olivine.

the different species detected. The product species have been grouped as follow: syngas species (CO, CO<sub>2</sub>, CH<sub>4</sub>) that can be used as fuel or in further synthesis processes; hydrocarbons that are directly recovered; and aromatic compounds. Note that the carbon content of the detected aromatic species which were labelled as *unknown* aromatic compounds in Fig. 6 is not known with certitude. However, for the sake of a more accurate calculation of the carbon balance, the carbon in the unknown aromatic compounds was estimated. The estimation was done by attributing to each unknown specie the average properties of the known aromatic species detected by the GC-FID before and after the *unknown* peak. The total carbon measured in the product stream represents a carbon balance closure of 73%, 78% and 84% for Day 1, Day 2, and Day 3, respectively. This leaves a significant fraction of undetected carbon, which decreases as the activation of the olivine proceeds.

As activation proceeds, the carbon of the feedstock that converts into CH<sub>4</sub> remains unaffected, and that in the C<sub>2</sub> + C<sub>3</sub> species increases slightly, which is due to the increase in C<sub>3</sub> compounds (recall Fig. 4). The

percentage changes of the carbon distribution when comparing Day 2 to Day 1 and Day 3 to Day 2 are summarized in Fig. 8. Larger changes in carbon distribution are observed for the carbon oxides, the aromatic compounds and the undetected carbon. These changes are more pronounced as the olivine gets more active. At the first stage of activation (Day 1 to 2), the carbon distribution shifts from the aromatic and undetected fractions mainly to C<sub>2</sub>-C<sub>3</sub> compounds and carbon oxides. Later on (Day 2 to Day 3), the carbon distribution shifts predominantly from the aromatic and undetected fraction to carbon oxides and to C<sub>2</sub>-C<sub>3</sub> compounds to some extent.

The content of the undetected carbon fraction may be solid carbon (e.g., soot, carbon deposits or char) or hydrocarbons that were out of the scope of the analytical methods applied. Previous works on steam cracking of similar feedstocks in fluidized bed have reported that <1% C of the carbon in the feedstock becomes carbon deposits at the operating temperature applied [39]. Taking into account the catalytic action of the ash layer that is present in this work, it is expected that the carbon that

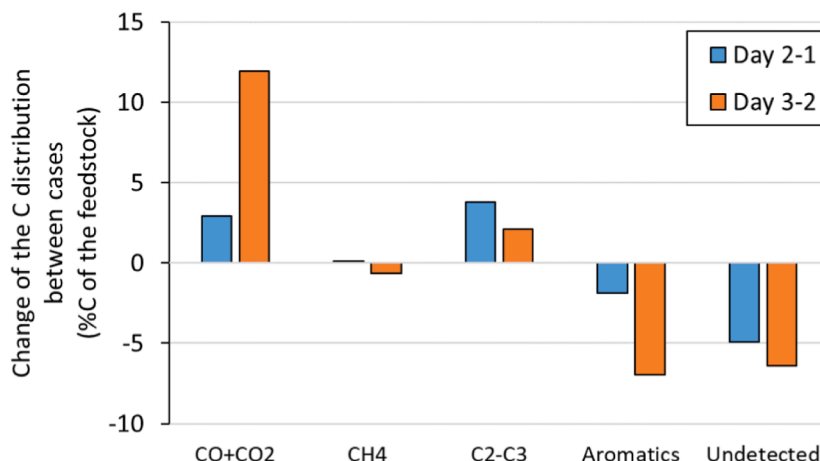


Fig. 8. Variation of the distribution of the carbon into gasification products during the aging process of olivine.

remains in solid form is even less important as the ash coated olivine can also catalyse steam gasification reactions [31]. Therefore, it is likely that the undetected fraction consists mainly of hydrocarbons with C<sub>4</sub> or heavier hydrocarbons which were not covered by the analytical methods applied in this work. To further elucidate the nature of the undetected fraction, hydrogen and oxygen balances are also analysed in the next section.

### 3.3. Elemental hydrogen and oxygen balances

In Fig. 9, the hydrogen distribution in the different products obtained is shown. The measured species (C<sub>2</sub>-C<sub>3</sub>, CH<sub>4</sub>, BTXS, other aromatics, and H<sub>2</sub>) represent a hydrogen balance closure of 85%, 92% and 105% for Day 1, Day 2 and Day 3, respectively. This analysis shows two points that will be discussed on the following. Firstly, that in Day 3, steam has certainly reacted with the feedstock since the overall hydrogen balance surpasses 100% only considering the measured compounds. Secondly, it confirms that the undetected fraction must be rich in hydrocarbons rather than on pure carbon particles (e.g., soot, carbon deposits), since there is hydrogen left in such fraction.

Assuming that the undetected fraction contains a mix of hydrocarbons with an average H/C ratio of 1.5, the hydrogen balance can be complemented with the rightmost bar in Fig. 9, which shows an estimate of the hydrogen in the undetected fraction. The choice of H/C = 1.5 in this analysis is based on the average of the possible H/C ratios which fulfil simultaneously the hydrogen and the oxygen balances, as explained below.

The oxygen balance results are summarized in Fig. 10, where the moles of oxygen atoms accounted in the product stream is shown as a dark blue line. The major species containing oxygen atoms in the gas are CO and CO<sub>2</sub>, some traces of phenolic compounds were also measured (See Fig. 6), yet their contribution to the oxygen balance is negligible. The oxygen found in the product streams, in the form of carbon oxides mainly, increases with the ash activation of the olivine from Day 1 to Day 3. This trend of increasing carbon oxides as activation proceeds is well in agreement with previous works with ash layered olivine and biomass [14,40].

The origin of the oxygen in the products can be attributed to two sources: reacted water through, e.g., steam reforming or water gas shift reaction, as well as to oxygen transport from the bed. Recall that the

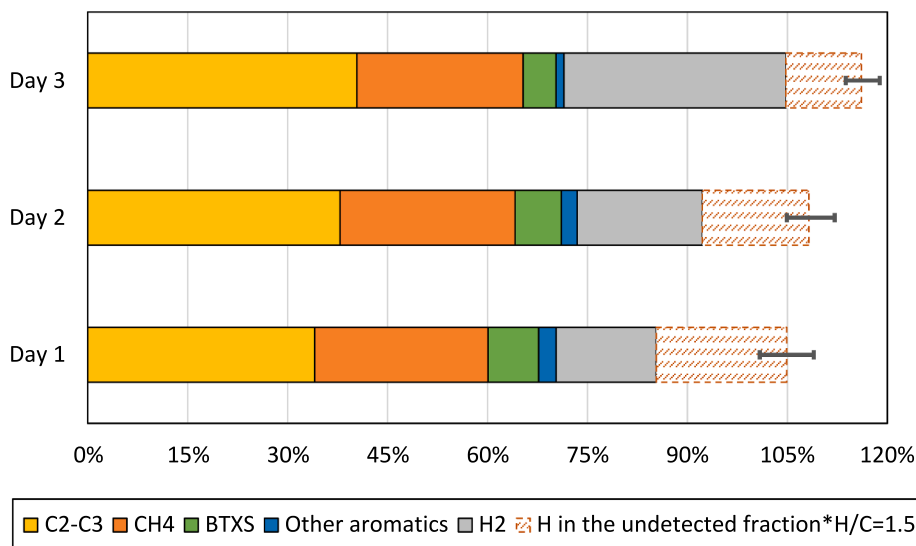


Fig. 9. Distribution of the hydrogen into gasification products during the aging process of olivine. Error bars represent the maximum (H/C = 1.8) and minimum (H/C = 1.2) H/C ratio in the undetected fraction.



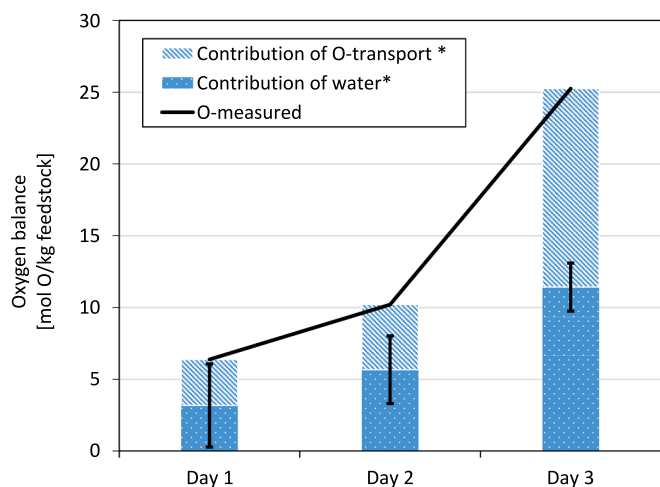


Fig. 10. Oxygen measured from the products generated during the aging process of olivine with the contributions of steam reactions and oxygen transport from the bed. Error bars represent the maximum ( $H/C = 1.75$ ) and minimum ( $H/C = 1.15$ )  $H/C$  ratio in the undetected fraction.

feedstock is free of oxygen and therefore it does not contribute to the oxygen balance. Two extreme cases can be envisioned regarding the origin of oxygen: that all the oxygen originates exclusively from oxygen transport of the bed or, alternatively, that all oxygen originates from reacted water. According to the molar balance calculations, the former implies that the  $H/C$  ratio of the undetected fraction is 1.2, while the latter implies a  $H/C$  ratio of 1.8 for the same product fraction. The error bars in Figs. 9-10 indicate all the possible solutions within these extreme cases ( $H/C = 1.2-1.8$ ).

Based on previous experiences with ash activated olivine, it is unlikely that all oxygen in the product stream originate exclusively from oxygen transport, i.e., extreme case of  $H/C = 1.2$ . In fact, with ash-activated olivine, the oxygen transport capability is limited given the low contents of transition metals in both the olivine and the biomass ash is rather low. Therefore, it is expected that the catalytic effect towards steam reactions predominates over the oxygen transport capability. This means that within the possible range of  $H/C$  ratios of the undetected fraction (1.2–1.8), it is most likely that the range is closer to 1.5 to 1.8. Such range of  $H/C$  ratio can correspond with an undetected fraction that consists of, e.g., a mixture of olefins and dienes of  $C_4$ – $C_6$  hydrocarbons; or a minor fraction of carbon deposits in combination with  $C_4$  and longer olefins. The results also imply that steam reactions such as steam reforming and the WGS play a role already from the early activation stage of the olivine (i.e., Day 1), which is well in line with the high yields of  $H_2$  and carbon oxides measured (recall Fig. 4). Nonetheless, further work with extended analytics is required to identify the specific compounds being part of this undetected fraction.

### 3.4. On the reaction paths promoted by ash enriched olivine

The changes of the permanent gas composition along with the reduction in aromatic species demonstrate a clear effect of the ash activated olivine on the conversion of olefinic cracking products. According to the results, the activation of the bed material gives a higher yield of permanent gases, mainly  $H_2$ ,  $CO$  and  $CO_2$ , at expenses of the yields of the total aromatic compounds and the undetected hydrocarbons. As discussed previously, such undetected fraction is most likely rich in  $C_4$  and larger olefins and dienes, which are fragments of the cracked original feedstock. These fragments may follow the conversion paths described in Fig. 1. They can further crack into smaller species such as  $CH_4$ ,  $C_2$  and  $C_3$ . In this case, a higher production of  $C_3$  compounds and  $C_2H_6$  was observed as the catalytic activity of the bed increased. Among the light hydrocarbon products,  $CH_4$  and  $C_2H_4$  were

the most abundant at the conditions tested, in line with their known stability [41]. Alternatively, the initial cracked products can follow the aromatization reaction path, which involves dehydrogenation and cyclization [42]. This aromatization path is also clear in the experiments conducted, by which benzene was the most abundant aromatic specie. The aromatization path was less pronounced as the catalytic activity increases, i.e., from Day 1 to 3.

It is remarkable the high yield of  $H_2$  generated in this investigation. Dehydrogenation reactions that form aromatic compounds can be responsible for  $H_2$  formation [42], as well as severe cracking of hydrocarbons into carbon deposits and  $H_2$ . However, the results indicate that large amounts of carbon deposits are not expected in this work, as previously discussed. It is inferred that at the conditions applied, a large share of the  $H_2$  originates instead from reactions involving steam. Accordingly, it is proposed that the earlier hydrocarbon fragments ( $\geq C_4$ ) also follow a steam reforming path. In fact, they convert preferentially into carbon oxides and  $H_2$  as the activation of the olivine proceeds. The concurrent lower yield of aromatic compounds observed as the olivine activates is here interpreted as a consequence of the steam reforming of this earlier cracking products. In other words, by steam reforming of the earlier olefinic cracking fragments, the subsequent aromatization of such species is avoided.

Overall, the treatment of olefinic rich feedstocks in combination with woody biomass will inevitably lead to a situation where the catalytic and oxygen transport effect of the ash plays a role on the feedstock conversion. With bed materials that are prone to develop marked catalytic properties by means of a biomass ash layer, it is expected that the yield of syngas will increase in the final product. Consequently, a larger share of the carbon in the feedstock can be expected become carbon oxides ( $CO$  and  $CO_2$ ) when the cracking of olefinic feedstocks occurs in the presence of biomass ash in DFB systems. The advantage or disadvantage of using ash activated bed materials depend on the final purpose of the process. For instance, if the aim is to recover as much valuable olefins and light aromatic compounds at the cracker reactor stage, the catalytic ash layer does not give any significant benefit in terms of direct recovery of chemical building blocks. This is due to the prevented aromatization path in combination with a mild decrease of the most abundant olefin in the product distribution, i.e.,  $C_2H_4$ . If the focus is on olefins production and the thermal recycling plant is equipped with a synthesis process that can convert the syngas into olefins, the use of ash activated bed materials can be of interest. In such scenario, the production of aromatics is limited at the expenses of syngas. Part of the olefins will be directly recovered at the cracker stage and additional olefins can be produced by synthesis.

## 4. Summary and conclusions

Herein, the effect of the exposure of olivine to biomass ash on cracking and aromatization of olefinic cracking products was assessed in the Chalmers dual fluidized bed gasifier. The changes of the permanent gas composition along with the reduction in aromatic species with the time of exposure demonstrate a clear effect of the ash activated olivine on the conversion of olefinic cracking products. The following conclusions can be drawn from this work:

- The production of syngas species (mainly  $H_2$ ,  $CO$  and  $CO_2$ ) was promoted by the ash activation of the olivine bed at expenses of the yields of the total aromatic compounds and the undetected hydrocarbons.
- The undetected fraction is a blend of hydrocarbons with a  $H/C$  ratio in the range of 1.5–1.8. The actual composition of this fraction could not be derived from this investigation and further work is required to identify its main species.
- These unknown compounds can crack into smaller species such as  $CH_4$ ,  $C_2$  and  $C_3$ , or they can alternatively follow an aromatization reaction path involving dehydrogenation and cyclization. The results

indicate that such fraction follows a steam reforming route rather than aromatization paths as the activation of the olivine proceeds.

These aspects are crucial to understand the effect of in-bed catalysis by biomass ash during steam cracking of linear hydrocarbons in DFB systems. This work shows the consequences of ash activation on the cracking product distribution at a cracking temperature of 780–790 °C, where the ash-coated olivine promotes the steam reforming of early aromatic precursors. The results suggest opportunities to increase the yields of valuable olefins and light aromatics by limiting the catalytic activation of the bed.

### CRedit authorship contribution statement

**Judith González-Arias:** Conceptualization, Methodology, Investigation, Data curation, Writing – original draft. **Teresa Berdugo-Vilches:** Conceptualization, Methodology, Investigation, Data curation, Visualization, Writing – review & editing. **Chahat Mandviwala:** Methodology, Investigation, Writing – review & editing. **Isabel Cañete-Vela:** Investigation, Visualization. **Martin Seemann:** Supervision, Project administration, Funding acquisition. **Henrik Thunman:** Writing – review & editing, Project administration, Funding acquisition.

### Declaration of Competing Interest

The authors declare that they have no known competing financial interests or personal relationships that could have appeared to influence the work reported in this paper.

### Data availability

Data will be made available on request.

### Acknowledgments

This work was supported financially by Borealis AB and the Swedish Energy Agency (Project number: 49514–1), the Swedish Gasification Centre (SFC), and the European Commission (Project ID: EC/H2020/951308).

### References

- [1] Kaminsky W. The hamburg fluidized-bed pyrolysis process to recycle polymer wastes and tires. In: Feedstock recycling and pyrolysis of waste plastics: converting waste plastics into diesel and other fuels; 2006. <https://doi.org/10.1002/0470021543.ch17>.
- [2] Thunman H, Berdugo Vilches T, Seemann M, Maric J, Vela IC, Pissot S, et al. Circular use of plastics-transformation of existing petrochemical clusters into thermochemical recycling plants with 100% plastics recovery. *Sustainable Mater Technol* 2019;22. <https://doi.org/10.1016/j.susmat.2019.e00124>.
- [3] Zhu HL, Zhang YS, Materazzi M, Aranda G, Brett DJL, Shearing PR, et al. Co-gasification of beech-wood and polyethylene in a fluidized-bed reactor. *Fuel Process Technol* 2019;190. <https://doi.org/10.1016/j.fuproc.2019.03.010>.
- [4] Wilk V, Hofbauer H. Co-gasification of plastics and biomass in a dual fluidized-bed steam gasifier: Possible interactions of fuels. *Energy Fuel* 2013;27. <https://doi.org/10.1021/ef400349k>.
- [5] Narobe M, Golob J, Klinar D, Francetić V, Likozar B. Co-gasification of biomass and plastics: Pyrolysis kinetics studies, experiments on 100kW dual fluidized bed pilot plant and development of thermodynamic equilibrium model and balances. *Bioresour Technol* 2014;162. <https://doi.org/10.1016/j.biortech.2014.03.121>.
- [6] Berdugo Vilches T, Marinkovic J, Seemann M, Thunman H. Comparing Active Bed Materials in a Dual Fluidized Bed Biomass Gasifier: Olivine, Bauxite, Quartz-Sand, and Ilmenite. *Energy Fuel* 2016;30. <https://doi.org/10.1021/acs.energyfuels.6b00327>.
- [7] Kirnbauer F, Wilk V, Kitzler H, Kern S, Hofbauer H. The positive effects of bed material coating on tar reduction in a dual fluidized bed gasifier. *Fuel* 2012;95. <https://doi.org/10.1016/j.fuel.2011.10.066>.
- [8] Marinkovic J. Choice of bed material: a critical parameter in the optimization of dual fluidized bed systems. *Chalmers University of Technology*; 2016.
- [9] Berguerand N, Berdugo VT. Alkali-Feldspar as a Catalyst for Biomass Gasification in a 2-MW Indirect Gasifier. *Energy Fuel* 2017;31. <https://doi.org/10.1021/acs.energyfuels.6b02312>.
- [10] Zevenhoven-Onderwater M, Öhman M, Skrifvars BJ, Backman R, Nordin A, Hupa M. Bed agglomeration characteristics of wood-derived fuels in FBC. *Energy Fuel* 2006;20. <https://doi.org/10.1021/ef050349d>.
- [11] Kuba M, He H, Kirnbauer F, Skoglund N, Boström D, Öhman M, et al. Mechanism of layer formation on olivine bed particles in industrial-scale dual fluid bed gasification of wood. *Energy Fuel* 2016;30. <https://doi.org/10.1021/acs.energyfuels.6b01522>.
- [12] Kirnbauer F, Hofbauer H. The mechanism of bed material coating in dual fluidized bed biomass steam gasification plants and its impact on plant optimization. *Powder Technol* 2013;245. <https://doi.org/10.1016/j.powtec.2013.04.022>.
- [13] Vilches TB. Operational strategies to control the gas composition in dual fluidized bed biomass gasifiers. *Chalmers University of Technology*; 2018.
- [14] Pissot S, Berdugo Vilches T, Thunman H, Seemann M. Effect of ash circulation on the performance of a dual fluidized bed gasification system. *Biomass Bioenergy* 2018;115:45–55. <https://doi.org/10.1016/j.biombioe.2018.04.010>.
- [15] Larsson A, Kuba M, Berdugo Vilches T, Seemann M, Hofbauer H, Thunman H. Steam gasification of biomass – Typical gas quality and operational strategies derived from industrial-scale plants. *Fuel Process Technol* 2021;212. <https://doi.org/10.1016/j.fuproc.2020.106609>.
- [16] Koppatz S, Pfeifer C, Hofbauer H. Comparison of the performance behaviour of silica sand and olivine in a dual fluidised bed reactor system for steam gasification of biomass at pilot plant scale. *Chem Eng J* 2011;175. <https://doi.org/10.1016/j.cej.2011.09.071>.
- [17] Marinkovic J, Thunman H, Knutsson P, Seemann M. Characteristics of olivine as a bed material in an indirect biomass gasifier. *Chem Eng J* 2015;279. <https://doi.org/10.1016/j.cej.2015.05.061>.
- [18] Berdugo Vilches T, Seemann M, Thunman H. Influence of In-Bed Catalysis by Ash-Coated Olivine on Tar Formation in Steam Gasification of Biomass. *Energy Fuel* 2018;32. <https://doi.org/10.1021/acs.energyfuels.8b02153>.
- [19] Kouinke FD, Zimmermann G, Ondruschka B. Tendencies of Aromatization in Steam Cracking of Hydrocarbons. *Ind Eng Chem Res* 1987;26. <https://doi.org/10.1021/ie00071a037>.
- [20] Diaz-Silvarrey LS, Zhang K, Phan AN. Monomer recovery through advanced pyrolysis of waste high density polyethylene (HDPE). *Green Chem* 2018;20. <https://doi.org/10.1039/c7gc03662k>.
- [21] Gholami Z, Gholami F, Tisler Z, Vakili M. A review on the production of light olefins using steam cracking of hydrocarbons. *Energies (Basel)* 2021;14. <https://doi.org/10.3390/en14238190>.
- [22] Montaudo G, Puglisi C, Rapisardi R, Samperi F. Further studies on the thermal decomposition processes in polycarbonates. *Polym Degrad Stab* 1991;31. [https://doi.org/10.1016/0141-3910\(91\)90078-6](https://doi.org/10.1016/0141-3910(91)90078-6).
- [23] Bockhorn H, Hornung A, Hornung U. Mechanisms and kinetics of thermal decomposition of plastics from isothermal and dynamic measurements. *J Anal Appl Pyrolysis* 1999;50. [https://doi.org/10.1016/S0165-2370\(99\)00026-1](https://doi.org/10.1016/S0165-2370(99)00026-1).
- [24] Poutsma ML. Fundamental reactions of free radicals relevant to pyrolysis reactions. *J Anal Appl Pyrolysis* 2000;54. [https://doi.org/10.1016/S0165-2370\(99\)00083-2](https://doi.org/10.1016/S0165-2370(99)00083-2).
- [25] Sadrameli SM. Thermal/catalytic cracking of hydrocarbons for the production of olefins: A state-of-the-art review I: Thermal cracking review. *Fuel* 2015;140. <https://doi.org/10.1016/j.fuel.2014.09.034>.
- [26] Chauvel A, Lefebvre G. Petrochemical Processes. Technical and economic characteristics. I Synthesis-gas derivatives and mayor hydrocarbons 1989. [https://books.google.se/books?hl=es&lr=&id=em2RH6lg66oC&oi=fnd&pg=PR7&ots=9\\_oOCAvGAE&sig=\\_A17ELg3HfL0kjcLJl0Xnksxnl&redir\\_esc=y#v=onepage&q&f=false](https://books.google.se/books?hl=es&lr=&id=em2RH6lg66oC&oi=fnd&pg=PR7&ots=9_oOCAvGAE&sig=_A17ELg3HfL0kjcLJl0Xnksxnl&redir_esc=y#v=onepage&q&f=false) (accessed August 22, 2022).
- [27] Chen NY, Yan TY. M2 forming a process for aromatization of light hydrocarbons. *Industrial and Engineering Chemistry Process Design and Development* 1986;25. <https://doi.org/10.1021/i200032a023>.
- [28] Isagulyants G, v., Dubinskii, YG., Rozengart, MI.. The Mechanism of the Aromatization of Paraffinic Hydrocarbons on Oxide Catalysts. *Russ Chem Rev* 1981;50. <https://doi.org/10.1070/rc1981v050n09abeh002687>.
- [29] Song Y, Zhu X, Xie S, Wang Q, Xu L. The effect of acidity on olefin aromatization over potassium modified ZSM-5 catalysts. *Catal Letters* 2004;97. <https://doi.org/10.1023/B:CATL.0000034281.58853.76>.
- [30] Kuba M, Kirnbauer F, Hofbauer H. Influence of coated olivine on the conversion of intermediate products from decomposition of biomass tars during gasification. *Biomass Convers Biorefin* 2017;7. <https://doi.org/10.1007/s13399-016-0204-z>.
- [31] Berdugo Vilches T, Maric J, Knutsson P, Rosenfeld DC, Thunman H, Seemann M. Bed material as a catalyst for char gasification: The case of ash-coated olivine activated by K and S addition. *Fuel* 2018;224. <https://doi.org/10.1016/j.fuel.2018.03.079>.
- [32] Kuba M, Fürsatz K, Janisch D, Aziaba K, Chlebda D, Łojewska J, et al. Surface characterization of ash-layered olivine from fluidized bed biomass gasification. *Biomass Convers Biorefin* 2021;11. <https://doi.org/10.1007/s13399-020-00863-2>.
- [33] Faust R, Sattari M, Maric J, Seemann M, Knutsson P. Microscopic investigation of layer growth during olivine bed material aging during indirect gasification of biomass. *Fuel* 2020;266. <https://doi.org/10.1016/j.fuel.2020.117076>.
- [34] Larsson A, Seemann M, Neves D, Thunman H. Evaluation of performance of industrial-scale dual fluidized bed gasifiers using the chalmers 2–4-MWth gasifier. *Energy Fuel* 2013;27. <https://doi.org/10.1021/ef400981j>.
- [35] Israelsson M, Seemann M, Thunman H. Assessment of the solid-phase adsorption method for sampling biomass-derived tar in industrial environments. *Energy Fuel* 2013;27. <https://doi.org/10.1021/ef401893j>.
- [36] Hannl TK, Faust R, Kuba M, Knutsson P, Berdugo Vilches T, Seemann M, et al. Layer Formation on Feldspar Bed Particles during Indirect Gasification of Wood. 2.

- Na-Feldspar. *Energy Fuel* 2019;33. <https://doi.org/10.1021/acs.energyfuels.9b01292>.
- [37] Devi L, Ptasiński KJ, Janssen FJJG, van Paasen SVB, Bergman PCA, Kiel JHA. Catalytic decomposition of biomass tars: Use of dolomite and untreated olivine. *Renew. Energy* 2005;30. <https://doi.org/10.1016/j.renene.2004.07.014>.
- [38] Kirnbauer F, Hofbauer H. Investigations on bed material changes in a dual fluidized bed steam gasification plant in Güssing. *Austria Energy and Fuels* 2011;25. <https://doi.org/10.1021/ef200746c>.
- [39] Mandviwala C, Vilches Berdugo T, Seemann M, González-Arias J, Thunman H. Unraveling the hydrocracking capabilities of fluidized bed systems operated with natural ores as bed materials. *J Anal Appl Pyrolysis* 2022;166:105603. <https://doi.org/10.1016/j.jaap.2022.105603>.
- [40] Pissot S, Faust R, Aonsamang P, Berdugo Vilches T, Maric J, Thunman H, et al. Development of oxygen transport properties by olivine and feldspar in industrial-scale dual fluidized bed gasification of woody biomass. *Energy Fuel* 2021;35. <https://doi.org/10.1021/acs.energyfuels.1c00586>.
- [41] Faravelli T, Bozzano G, Scassa C, Perego M, Fabini S, Ranzi E, et al. Gas product distribution from polyethylene pyrolysis. *J Anal Appl Pyrolysis* 1999;52. [https://doi.org/10.1016/S0165-2370\(99\)00032-7](https://doi.org/10.1016/S0165-2370(99)00032-7).
- [42] Mastral FJ, Esperanza E, Berruero C, Juste M, Ceamanos J. Fluidized bed thermal degradation products of HDPE in an inert atmosphere and in air-nitrogen mixtures. *J Anal Appl Pyrolysis* 2003;70. [https://doi.org/10.1016/S0165-2370\(02\)00068-2](https://doi.org/10.1016/S0165-2370(02)00068-2).